VU Research Portal

Imaging the structure and the movement of the retina with scanning light ophthalmoscopy

Vienola, K.V.

2018

document version
Publisher's PDF, also known as Version of record

Link to publication in VU Research Portal

citation for published version (APA)
Vienola, K. V. (2018). *Imaging the structure and the movement of the retina with scanning light ophthalmoscopy*.
[PhD-Thesis - Research and graduation internal, Vrije Universiteit Amsterdam].

6

General discussion and outlook

Introduction to the discussion

In this thesis, SLOs were used and developed to detect the fixational eye movements that naturally occur during our vision process. With the experimental SLO systems (chapters 3 and 4) these movements can be extracted from the retinal images as the imaging speed is high enough to record them. In chapter 3 the benefits of the eye-tracking are shown in SS-OCT and Doppler OCT where the image quality is significantly improved compared to non-tracked counterparts. The DMD-based ophthalmoscopes were designed and built (chapters 4 and 5) to address some of the limitations discovered in the earlier implementation with the scanning spot SLO (TSLO). This resulted in novel ophthalmoscopes that were able to visualize the retina with confocal images and perform proof-of-principle motion detection measurements in healthy individuals *in vivo*.

As there are already elaborate chapter specific discussions, this chapter focuses on the technical prospects and key elements that will be crucial for the future development of the real-time eye motion detection. Additionally technologies that can be brought to retinal imaging with the use of eye tracking are presented. Finally the thesis conclusions are given with closing remarks.

6.1 Field-programmable gate arrays for data acquisition and processing

The field-programmable gate arrays (FPGAs) have become increasingly popular after their commercialization in 1985 [1]. Essentially, FPGAs are reprogrammable silicon chips where you can reprogram the functionality without changing anything in the hardware itself. Whereas in traditional digital signal processors (DSPs) computations happen sequentially, in FPGA they happen in parallel which leads to higher computing powers. Controlling the inputs and outputs lets the user to decide when the central processing unit (CPU) is needed, minimizing the data swapping between the data acquisition card and CPU for example. This allows much faster data processing and the time difference between input and output can be as fast as 40 MHz or 25 ns [2].

The FPGA consists of an array of logic blocks (configurable and fixed ones), routing channels and I/O pads [2]. The configurable logic blocks (CLBs) consists of two basic components called flip-flops and lookup tables (LUTs). The flip-flops function as binary shift registers saving the logical states between clock cycles in order to synchronize logic. LUT is, as the name suggests, a table that determines what the output will be for any given input(s), instead of having logic gates such as AND or NOR, LUTs are used in FPGA [3]. The programming of an FPGA board used to be a tedious task and required expertise in hardware description languages such as VHSIC hardware description language (VHDL). However, since 2003 National instruments have supported FPGA programming with their visual programming language in LabVIEW, enabling easier implementation of FPGAs to measurements systems by novice users.

For real-time image-based eye tracking, having an FPGA for signal processing and image acquisition should be considered as it brings many advantages. Firstly the data acquisition can be customized. This means that instead of *e.g.* buying a frame grabber, it will be programmed to the FPGA enabling full control of the data flow from the detector/camera. Secondly, the DSP can be implemented in the FPGA which can significantly decrease the latency as the computer doesn't have to wait for the data to be acquired but it can start to process it in parallel with the acquisition. And this is an extremely important thing to consider when thinking about eye-tracking as auxiliary device for other ophthalmic systems as it needs to deliver the motion correction signal in real time in order to be accurate and precise.

6.2 The effect of latency to tracking bandwidth

In real-time eye tracking, the latency can be defined as the time interval between the motion occurring in the eye and the time point when that motion is corrected. In image-based systems such as the TSLO or the PLSO, the latency is a combination of two things: data acquisition and the signal processing time. Also depending on the implementation, the response time of the system that is being corrected can be also included. The effect of latency can be simulated with two sinusoidal waveforms, one being the input motion $f_i(t)$ and $f_o(t)$ the output motion. The simulated input sine wave is the motion that is being detected (like the natural eye motion) and can be expressed as

$$f_i(t) = A_1 \sin(2\pi f t), \tag{6.1}$$

where A_1 is the amplitude of the sine wave, f the frequency and t the time in seconds. The output sinusoidal wave (the correction signal) is otherwise the same but has the latency factor:

$$f_o(t) = A_2 \sin(2\pi f(t - t_{\text{lag}})), \tag{6.2}$$

with A_2 being the amplitude of the output sine wave and t_{lag} the latency. As the image acquisition and processing needs at least some time, there is always some error in the correction signal. By subtracting the output from the input wave and assuming that the amplitude remains the same ($A_1 = A_2 = 1$), a residual motion wave $f_r(t)$ is obtained:

$$f_r(t) = f_i(t) - f_o(t) = \sin(2\pi f t) - \sin(2\pi f(t - t_{\text{lag}})). \tag{6.3}$$

By using the trigonometric subtraction formula for sine, equation 6.3 becomes

$$f_r(t) = 2 \sin(\pi f t_{\text{lag}}) \cos(\pi f (2t - t_{\text{lag}})). \tag{6.4}$$

These waves are simulated in Fig. 6.1A where the residual motion wave is seen in yellow. For this particular simulation the frequency was set to 10 Hz and the latency to 2.5 ms. It is clear that even small latency has a big impact on the correction signal as they increase the sine term in Eq. 6.4. The amplitude of the residual motion wave $f_r(t)$ can be regarded as the tracking error. If the correction would be perfect, $f_r(t)$ would be zero. This error is further illustrated in Fig. 6.1B where the tracking error is shown as a function of latency for three different frequencies.

As the latency is a combination of the image acquisition and processing, it is therefore reasonable to assume that it will always be larger than 0 ms. As the tracking
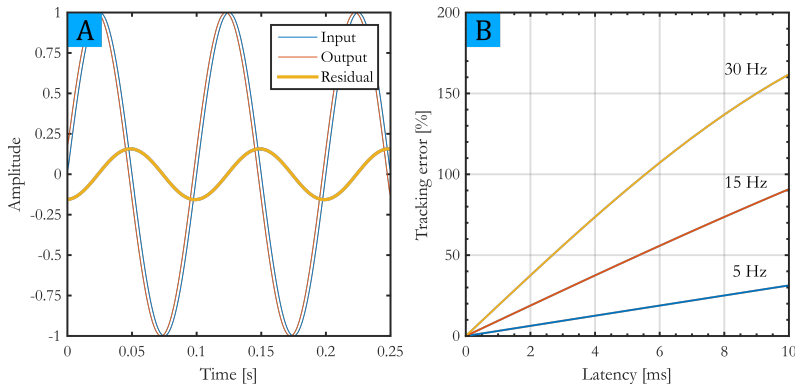
Figure 6.1: Tracking error simulation with sinusoidal waveforms. (A) Input and output signals are almost overlapping in the plot but they have 2.5 ms latency between them. This means that they don't cancel each other perfectly and the residual signal can be seen as yellow. For tracking this means that only about 80% of the amplitude is corrected. (B) Here tracking error is plotted as a function of latency for three different frequencies. It is easily seen that for frequencies above 5 Hz, the error increases rapidly when the latency is above 2 ms.

error increases much faster with higher frequencies, it is therefore desirable to have the latency low as possible to be able to correct higher frequencies with minimal error. In chapter 3, the effect of latency is highly visible, as the system has an eye motion reporting rate of 960 Hz, but is only able to have a tracking bandwidth of 32 Hz, when considering 50% tracking error as the limit.

It is noteworthy to mention that a tracking bandwidth of 50 Hz is decent for counteracting micro-saccades and drift and most of the tremor and the effect of high frequency tremor only comes to play with small FOV used in AOSLOs where the resolution is so high that individual cones are visualized.

6.3   Accuracy in image-based motion detection

As the human eye is always moving, it is hard to determine the accuracy of the motion detection as there is no "ground truth" available. It can be that the magnification in the system is designed in a way that the single pixel shift can either be contributed to system noise or to tremor. This means that the reference image used in image-based tracking has always some motion encoded in the image. If the distortion is big enough, it can cause visible distortions throughout the whole dataset as all of the data is cross-correlated to the reference frame. This is something that most researchers in the field are aware of. It hasn't been a real issue as the SLO produces frames at 30 Hz and the operator can always continue selecting a new frame from the video feed until a good reference frame is obtained. Good meaning no visible distortions in this case [4]. Recently a few publications have tackled this issue.

Salmon *et al.* presented their automated reference frame selection (ARFS) algorithm to remove the subjectivity from the reference frame selection and eliminate operator bias. Although the ARFS didn't outperform the strip-based method, it is a promising advancement when the AOSLO systems are brought from the laboratory to a clinical environment.

As the fixational eye movement is random, the only method to avoid it in the reference frame is to image faster. Bedggood and Metha used an AO flood illumination system to obtain a reference frame that has minimal intra-frame distortions due to a 2.5 ms exposure time [5]. They were then able to simulate motion in the frames and assess different methods for motion recovery and showed that minimizing the reference frame distortions do have an impact on the accuracy itself. By using flood illumination to generate the reference frame, acquisition time is decreased by a factor of ten compared to raster-scanning. Another option is to use a line illumination instead of a spot which effectively eliminates one scanning mirror and allows faster imaging [6, 7]. As expected, Lu *et al.* reported a decrease in intra-frame distortions when increasing the image speed from 30 Hz to 200 Hz. However, it is also seen that the image quality, especially the contrast of the image, decreases, making the eye motion trace noisier.

In order to improve the accuracy of image-based eye tracking, there are two options when assuming that the normalized cross-correlation (NCC) peak localization is already accurate. One is to chance the optical components used in the system to improve the resolution of the images. This means that the area imaged remains the same, but it is now mapped (sampled) with smaller pixels. The second option is to change the NCC peak detection algorithm to detect subpixel changes. These methods include doing zero-padding before the fast Fourier transform (FFT) and detecting the center of the mass in the NCC matrix, for example. These two options can be also both implemented at the same time but the latter one is usually much easier to implement on all platforms. Having tracking accuracy ≤ 1 μm is already below the reported amplitude of tremor component (and photoreceptor diameter in the fovea) and this can be achieved with either of the proposed software approaches.

6.4   New opportunities for real-time eye tracking

Techniques such as optical coherence tomography have become so advanced, that their imaging speed can be already described as volumes per second. It is so fast that there is no time for eye motion to occur when doing structural imaging. That doesn't mean that motion detection isn't useful for OCT. As everything has to do with sampling rate, it is true that standard C-scans can be acquired within 1-2 seconds, but

that doesn't mean that eye tracking is becoming obsolete. Even with OCT eye tracking becomes important, when moving to ultra-widefield imaging (over 100 degrees), as the acquisition time can be 8 seconds or more [8]. Another good application where eye tracking can be beneficial is Doppler OCT, or as it is better known among clinicians, OCT angiography (OCTA). Whether the method to detect the blood flow is with amplitude decorrelation [9], speckle variance [10, 11] or phase variance [12, 13], averaging of the volumes is always crucial to produce a good quality angiograms.

The benefits of motion detection are not limited to OCT, as there are other emerging technologies that actually need tracking to be able to produce meaningful *in vivo* data in ophthalmology. One such technology is two-photon fluorescence ophthalmoscopy [14, 15] where *in vivo* imaging of the retina is still to be realized. To get enough fluorescence back to the detector, either the illumination has to be very powerful or long integration times are needed. As the wavelength used for two-photon imaging is quite short, the amount of optical power that can be sent to the eye is very limited. With eye tracking the integration time can be increased and the optical power can be kept within the safety limits.

Another imaging technique that can benefit from motion detection is Raman spectroscopy [16, 17] and its many variants such as stimulated Raman spectroscopy (SRS) [18, 19] or coherent anti-Stokes Raman spectroscopy (CARS) [20, 21]. For these methods, it is well known that when doing a spectral map of the sample (image), each data point (pixel) can take somewhere between 1 to 10 seconds. For a 64×64 image this would already mean acquisition times of 68 minutes or more. Obviously this means that any type of *in vivo* retinal imaging is not feasible as the eye motion renders the data useless and no localization is achieved. The usefulness of eye tracking can be easily realized here as it will keep the retinal image stabilized and the integration times can be kept high.

6.5 Thesis conclusion

SLO is a resourceful optical imaging modality for non-invasive high-resolution imaging of the retina. The chapters presented in this thesis showed that by carefully designing and building the SLO systems, they are very well suited for retinal imaging and for fixational eye movement detection. This allows correction of eye movement in the acquired datasets resulting averaged high-quality images and allowed even correction of secondary imaging system such as the Doppler OCT. The importance of effective eye-tracking is evident as older population does not have the same ability to fixate anymore, which leads to distortions in the datasets. By providing stable eye tracking over a large frequency range, it is expected that other imaging modali-

ties can be brought to ophthalmology such as Raman spectroscopy and two-photon fluorescence imaging.

6

References

[1] R. H. Freeman. Configurable electrical circuit having configurable logic elements and configurable interconnects. US Pattent 4,870,302, Sep. 1989.

[2] E. Monmasson and M. N. Cirstea. FPGA Design Methodology for Industrial Control Systems - A Review. *IEEE Trans. Ind. Electron.*, 54(4):1824–1842, 2007.

[3] S. Brown and J. Rose. FPGA and CPLD architectures: a tutorial. *IEEE Des. Test. Comput*, 13(2):42–57, 1996.

[4] R. F. Cooper, Y. N. Sulai, A. M. Dubis, T. Y. Chui, R. B. Rosen, M. Michaelides, A. Dubra, and J. Carroll. Effects of Intraframe Distortion on Measures of Cone Mosaic Geometry from Adaptive Optics Scanning Light Ophthalmoscopy. *Transl. Vis. Sci. Technol.*, 5(1):10–10, 2016.

[5] P. Bedggood and A. Metha. De-warping of images and improved eye tracking for the scanning laser ophthalmoscope. *PLoS ONE*, 12(4):e0174617, 2017.

[6] D. X. Hammer, R. H. Webb, R. D. Ferguson, T. E. Ustun, C. E. Bigelow, and N. V. Iftimia. Line-scanning laser ophthalmoscope. *J. Biomed. Opt.*, 11(4):041126–10, 2006.

[7] J. Lu, B. Gu, X. Wang, and Y. Zhang. High-speed adaptive optics line scan confocal retinal imaging for human eye. *PLoS ONE*, 12(3):e0169358, 2017.

[8] J. P. Kolb, T. Klein, C. L. Kufner, W. Wieser, A. S. Neubauer, and R. Huber. Ultra-widefield retinal MHz-OCT imaging with up to 100 degrees viewing angle. *Biomed. Opt. Express*, 6(5):1534–1552, 2015.

[9] Y. Jia, O. Tan, J. Tokayer, B. Potsaid, Y. Wang, J. J. Liu, M. F. Kraus, H. Subhash, J. G. Fujimoto, J. Hornegger, and D. Huang. Split-spectrum amplitude-decorrelation angiography with optical coherence tomography. *Opt. Express*, 20(4):4710–4725, 2012.

[10] A. Mariampillai, B. A. Standish, E. H. Moriyama, M. Khurana, N. R. Munce, M. K. K. Leung, J. Jiang, A. Cable, B. C. Wilson, I. A. Vitkin, and V. X. D. Yang. Speckle variance detection of microvasculature using swept-source optical coherence tomography. *Opt. Lett.*, 33(13):1530–1532, 2008.

[11] A. Mariampillai, M. K. K. Leung, M. Jarvi, B. A. Standish, K. Lee, B. C. Wilson, A. Vitkin, and V. X. D. Yang. Optimized speckle variance OCT imaging of microvasculature. *Opt. Lett.*, 35(8):1257–1259, 2010.

[12] B. Braaf, K. A. Vermeer, V. A. D. P. Sicam, E. van Zeeburg, J. C. van Meurs, and J. F. de Boer. Phase-stabilized optical frequency domain imaging at 1-µm for the measurement of blood flow in the human choroid. *Opt. Express*, 19(21):20886–20903, 2011.

[13] J. Fingler, D. Schwartz, C. Yang, and S. E. Fraser. Mobility and transverse flow visualization using phase variance contrast with spectral domain optical coherence tomography. *Opt. Express*, 15(20): 12636–12653, 2007.

[14] J. J. Hunter, B. Masella, A. Dubra, R. Sharma, L. Yin, W. H. Merigan, G. Palczewska, K. Palczewski, and D. R. Williams. Images of photoreceptors in living primate eyes using adaptive optics two-photon ophthalmoscopy. *Biomed. Opt. Express*, 2(1):139–148, 2011.

[15] J. A. Feeks and J. J. Hunter. Adaptive optics two-photon excited fluorescence lifetime imaging ophthalmoscopy of exogenous fluorophores in mice. *Biomed. Opt. Express*, 8(5):2483–2495, 2017.

[16] E. Smith and G. Dent. *Modern Raman Spectroscopy – A Practical Approach*. John Wiley & Sons, Ltd,

2005.

[17] C. V. Raman and K. S. Krishnan. The Optical Analogue of the Compton Effect. *Nature*, 121(3053): 711, 1928.

[18] C. W. Freudiger, W. Min, B. G. Saar, S. Lu, G. R. Holtom, C. He, J. C. Tsai, J. X. Kang, and X. S. Xie. Label-Free Biomedical Imaging with High Sensitivity by Stimulated Raman Scattering Microscopy. *Science*, 322(5909):1857–1861, 2008.

[19] M. J. B. Moester, F. Ariese, and J. F. de Boer. Optimized signal-to-noise ratio with shot noise limited detection in Stimulated Raman Scattering microscopy. *Journal of the European Optical Society Rapid Publications*, 10(15022), 2015.

[20] W. M. Tolles, J. W. Nibler, J. R. McDonald, and A. B. Harvey. A Review of the Theory and Application of Coherent Anti-Stokes Raman Spectroscopy (CARS). *Appl. Spectrosc.*, 31(4):253–271, 1977.

[21] A. M. Zheltikov. Coherent anti-Stokes Raman scattering: from proof-of-the-principle experiments to femtosecond CARS and higher order wave-mixing generalizations. *J. Raman Spectrosc.*, 31(8-9): 653–667, 2000.